

A Combined Adjustment of Geodetic and Photogrammetric Observations*

A three-dimensional geodetic mathematical model is combined with a photogrammetric bundle adjustment with self calibration.

INTRODUCTION

IN MOST of the phototriangulation solutions, the adjustment of photogrammetric and geodetic data is carried out in two sequential and separate steps. However, in some areas the available geodetic observations may not be sufficient for adjusting a geodetic network to provide the necessary control point coordinates for phototriangulation. Therefore, instead of using geodetically adjusted control point coordinates, the available observations are entered directly into a simultaneous adjustment with the photogrammetric measurements. This also has the advantage of providing a realistic approach to the problem of error analysis through weighting of all measured quantities.

ABSTRACT: The availability of highly accurate and dense control networks is a major requirement for large scale urban mapping, as well as for various engineering projects.

Although advanced photogrammetric systems have achieved a level of accuracy which makes their practical applications generally feasible, even in urban situations, additional data still can improve the results. Geodetic observations, even if they are not sufficient for a terrestrial network, provide excellent constraints to the photogrammetric adjustment and also reduce absolute control requirements. Although the idea of a simultaneous geodetic and photogrammetric adjustment is not new, the method used in this approach appears to be more rigorous as it does not rely on approximations. Here, a modern three-dimensional geodetic mathematical model is combined with a photogrammetric bundle adjustment with self calibration. A number of tests based on real as well as simulated data is presented in this paper.

The idea of a simultaneous adjustment is not new. The bundle adjustment program SAPGO (Wong and Elphingstone, 1971; Wong and Elphingstone, 1972) uses geodetic observations such as distances, angles, and azimuths as input to the photogrammetric solution. The geodetic observation equations, however, are those of classical geodesy, which treats horizontal and vertical adjustments separately, and performs the horizontal adjustment on the surface of a reference ellipsoid as a function of longitude and latitude. In order to combine these geodetic models with the photogrammetric ones, the geodetic observation equations were subjected to modifications in order to be expressed in the same coordinate system as the photogrammetric equations.

In this paper the combined solution is applied using the modern three-dimensional geodetic mathematical models (Vincenty, 1973). In this case the solution is carried out without any approximations or modification to the geodetic models to suit the photogrammetric models.

* Based on a paper titled "Combined Geodetic and Photogrammetric Adjustment for Densification of Control Networks," presented at the 45th ASP Annual Convention, Washington, DC, 18-24 March 1979.

THE MATHEMATICAL MODELS

FOR PHOTOGRAMMETRIC OBSERVATIONS

The photogrammetric mathematical model is the self-calibration bundle adjustment model:

$$x_A - x_o + dV_x = -f \left[\frac{(X_p - X_c)m_{11} + (Y_p - Y_c)m_{12} + (Z_p - Z_c)m_{13}}{(X_p - X_c)m_{31} + (Y_p - Y_c)m_{32} + (Z_p - Z_c)m_{33}} \right] \quad (1)$$

and

$$y_A - y_o + dV_y = -f \left[\frac{(X_p - X_c)m_{21} + (Y_p - Y_c)m_{22} + (Z_p - Z_c)m_{23}}{(X_p - X_c)m_{31} + (Y_p - Y_c)m_{32} + (Z_p - Z_c)m_{33}} \right]$$

where the correction terms dV_x and dV_y are given by (See El Hakim and Faig, 1977)

$$dV_x = (x_A - x_o) \cdot T \quad (2)$$

and

$$dV_y = (y_A - y_o) \cdot T.$$

with T being the harmonic function

$$T = a_{00} + a_{11} \cos \lambda + b_{11} \sin \lambda + a_{20}r + a_{22}r \cos 2\lambda + b_{22}r \sin 2\lambda + a_{31}r^2 \cos \lambda + b_{31}r^2 \sin \lambda + a_{33}r^2 \cos 3\lambda + b_{33}r^2 \sin 3\lambda + \dots \quad (3)$$

and

$$r = \sqrt{(x_A - x_o)^2 + (y_A - y_o)^2}$$

FOR GEODETIC OBSERVATIONS

The observation equations for the geodetic observations are based on modern three-dimensional geodesy (Fubara, 1972; Vincenty, 1973) in a Cartesian (x, y, z) coordinate system.

The observations accepted in this approach are slope distances, vertical angles, horizontal directions, astronomic azimuths, elevation differences, astronomic longitudes, and astronomic latitudes.

For the work reported in this paper the equations had to be transferred into a Cartesian coordinate system to suit combination with the photogrammetric models, and are given in linearized form, for each type of observable.

(1) Slope Distance, S_{ij} :

$$V_{s_{ij}} = C_1(dX_j - dX_i) + C_2(dY_j - dY_i) + C_3(dZ_j - dZ_i) + (S_c - S_o) \quad (4)$$

where

$$C_1 = (X_j - X_i)/S = \Delta X/S$$

$$C_2 = (Y_j - Y_i)/S = \Delta Y/S$$

$$C_3 = (Z_j - Z_i)/S = \Delta Z/S$$

where

S_c is computed from $(\Delta X^2 + \Delta Y^2 + \Delta Z^2)^{1/2}$ using approximate coordinates X, Y, Z of points i and j ; and where S_o is the observed value.

(2) Vertical Angles, β_{ij} :

$$V_{\beta_{ij}} = b_1(dX_j - dX_i) - b_2(dY_j - dY_i) + b_3(dZ_j - dZ_i) + b_4d\Phi_i + b_5d\Lambda_i - S_{ij}/10^3 \cdot dk_i + [\beta_c - (\beta_o - S_{ij}\cos\beta_{ij}k_i)] \quad (5)$$

where

$$b_1 = (S_{ij} \cdot \cos\Phi_i \cdot \cos\Lambda_i - \Delta X \sin\beta_{ij})/S_{ij}^2 \cdot \cos\beta_{ij}$$

$$b_2 = (S_{ij} \cdot \cos\Phi_i \cdot \cos\Lambda_i - \Delta Y \sin\beta_{ij})/S_{ij}^2 \cdot \cos\beta_{ij}$$

$$b_3 = (S_{ij} \cdot \sin\Phi_i - \Delta Z \cdot \sin\beta_{ij})/S_{ij}^2 \cdot \cos\beta_{ij}$$

$$b_4 = \cos\alpha_{ij}$$

$$b_5 = \cos\Phi_i \cdot \sin\alpha_{ij};$$

Φ and Λ are the astronomic latitude and longitude; and α is the astronomic azimuth.

The coefficient of refraction, k , can be made a function of the station, or a function of the line, or even a function of the direction. The initial value of k can be given as $0.13/2R$, where R is the mean radius of the Earth. β_c is computed from:

$$\beta_c = \sin^{-1} \frac{\Delta X \cos\Phi_i \cos\Lambda_i + \Delta Y \cos\Phi_i \sin\Lambda_i + \Delta Z \sin\Phi_i}{S_{ij}} \quad (6)$$

and

$$\alpha = \tan^{-1} \frac{\Delta Y \cos\Lambda_i - \Delta X \sin\Lambda_i}{\Delta Z \cos\Phi_i - \Delta X \sin\Phi_i \cos\Lambda_i - \Delta Y \sin\Phi_i \sin\Lambda_i} \quad (7)$$

The astronomic latitude and longitude, Φ and Λ , may not be available. However, because they appear as coefficients above, the corresponding geodetic latitude, ϕ , and longitude, λ , or any reasonable approximations can be substituted without significant loss of computational accuracy due to the fact that the solution is iterative. Thus, the initially approximate coefficients of the design matrices are improved with each iteration.

(3) Horizontal Direction, r_{ij} :

$$V_{r_{ij}} = a_1(dX_j - dX_i) + a_2(dY_j - dY_i) + a_3(dZ_j - dZ_i) + a_4d\Phi_i + a_5d\Lambda_i - dR_i + [\alpha_c - (r_{ij} + R_c)] \quad (8)$$

where

$$\begin{aligned} a_1 &= (\sin\alpha_{ij} \sin\Phi_i \cos\Lambda_i - \cos\alpha_{ij} \sin\Lambda_i) / S_{ij} \cos\beta_{ij}, \\ a_2 &= (\sin\alpha_{ij} \sin\Phi_i \sin\Lambda_i + \cos\alpha_{ij} \cos\Lambda_i) / S_{ij} \cos\beta_{ij}, \\ a_3 &= -\sin\alpha_{ij} \cos\Phi_i / S_{ij} \cos\beta_{ij}, \\ a_4 &= \sin\alpha_{ij} \tan\beta_{ij}, \\ a_5 &= \sin\Phi_i - \cos\alpha_{ij} \cos\Phi_i \tan\beta_{ij}, \end{aligned}$$

and α , Φ , Λ , and β are as previously defined. R_i is the initial azimuth or, in other words, the station orientation, and is usually treated as an unknown, with R_c as an approximation of it. β and α are computed from Equations 6 and 7, respectively.

(4) Astronomic Azimuth, α_{ij} :

$$V_{\alpha_{ij}} = a_1(dX_j - dX_i) + a_2(dY_j - dY_i) + a_3(dZ_j - dZ_i) + a_4d\Phi_i + a_5d\Lambda_i + [\alpha_c - \alpha_o] \quad (9)$$

where the coefficients are the same as in Equation 8, and α_c is the observed azimuth of the line i to j .

(5) Elevation Difference, ΔH_{ij} :

$$V_{\Delta H_{ij}} = e_1(dX_j - dX_i) + e_2(dY_j - dY_i) + e_3(dZ_j - dZ_i) + e_4d\Phi_i + e_5d\Lambda_i + e_6d\Phi_j + e_7d\Lambda_j + (\Delta h_c - \Delta H_o) \quad (10)$$

where

$$\begin{aligned} e_1 &= (S_{ij} \cos\Phi_i \cos\Lambda_i - \Delta X \sin\beta_{ij}) / 2S_{ij} \cos\beta_{ij} + (S_{ij} \cos\Phi_j \cos\Lambda_j - \Delta X \sin\beta_{ji}) / 2S_{ij} \cos\beta_{ji}; \\ e_2 &= (S_{ij} \cos\Phi_i \sin\Lambda_i - \Delta Y \sin\beta_{ij}) / 2S_{ij} \cos\beta_{ij} + (S_{ij} \cos\Phi_j \sin\Lambda_j - \Delta Y \sin\beta_{ji}) / 2S_{ij} \cos\beta_{ji}; \\ e_3 &= (S_{ij} \sin\Phi_i - \Delta Z \sin\beta_{ij}) / 2S_{ij} \sin\beta_{ij} + (S_{ij} \sin\Phi_j - \Delta Z \sin\beta_{ji}) / 2S_{ij} \cos\beta_{ji}; \\ e_4 &= (S_{ij} \cos\alpha_{ij}) / 2; \\ e_5 &= (S_{ij} \cos\Phi_i \sin\alpha_{ij}) / 2; \\ e_6 &= (S_{ij} \cos\alpha_{ji}) / 2; \\ e_7 &= (S_{ij} \cos\Phi_j \sin\alpha_{ji}) / 2; \end{aligned}$$

Δh_c is the assumed difference in ellipsoid height, when

$$\Delta h_c = 1/2 S(\beta_i - \beta_j);$$

with β_i and β_j being vertical angles as computed from Equation 6, and ΔH_o is the measured orthometric height.

(6) Astronomic Longitude, Λ_i :

$$V_{\Lambda_i} = d\Lambda_i + (\Lambda_c - \Lambda_o) \quad (11)$$

(7) Astronomic Latitude, Φ_i :

$$V_{\Phi_i} = d\Phi_i + (\Phi_c - \Phi_o) \quad (12)$$

In Equations 11 and 12, Λ_o and Φ_o are the observed quantities, while Λ_c and Φ_c are the computed values and can be taken as the geodetic longitude and latitude respectively.

THE COMBINED SOLUTION IN GENERAL TERMS

The photogrammetric model can be written as

$$F_p(\hat{X}_1, \hat{X}_2, L_p) = 0.0$$

or in linearized form:

$$W_p + A_{p1}\hat{X}_1 + A_{p2}\hat{X}_2 + B_p\hat{V}_p = 0.0 \quad (13)$$

where

- \hat{X}_1 is the vector of photo orientation elements and calibration parameters;
- \hat{X}_2 is the vector of object coordinates;
- L_p is the vector of observed photo coordinates;
- W_p is the misclosure vector = $F_p(X_1^0, X_2^0, L_p)$ where X_1^0 and X_2^0 are the initial values;
- \hat{V}_p is the vector of photo coordinates residuals; and
- A_{p1} , A_{p2} , and B_p are the design matrices, where

$$A_{p1} = \frac{\partial F_p}{\partial \hat{X}_1} / X_1^0, X_2^0, L_p; \quad A_{p2} = \frac{\partial F_p}{\partial \hat{X}_2} / X_1^0, X_2^0, L_p; \quad B_p = \frac{\partial F_p}{\partial L_p} / X_1^0, X_2^0, L_p$$

The geodetic model can be written as

$$F_g(\hat{X}_2, \hat{X}_3, L_g) = 0.0$$

or in linearized form:

$$W_g + A_{g1}\hat{X}_2 + A_{g2}\hat{X}_3 + B_g\hat{V}_g = 0.0 \quad (14)$$

where

- \hat{X}_3 is the vector of orientation, refraction unknowns, and astronomic coordinates;
- L_g is the vector of geodetic observations
- W_g is the misclosure vector = $F_g(X_2^0, X_3^0, L_g)$;
- \hat{V}_g is the vector of geodetic observation residuals; and
- A_{g1} , A_{g2} , and B_g are the design matrices.

The final solution is given by

$$\hat{X}_3 = -[Px_3 + Ng_{22}]^{-1} [Ug_2 + Ng_{21} \hat{X}_2] \quad (15)$$

$$\hat{X}_2 = -[Px_2 + Np_{22} + Ng_{11} - Ng_{12} (Px_3 + Ng_{22})^{-1} Ng_{21}]^{-1} \cdot [Up_2 + Ug_1 - Ng_{12} (Px_3 + Ng_{22})^{-1} Ug_2 + Np_{21} \hat{X}_1] \quad (16)$$

$$\hat{X}_1 = -[Px_1 + Np_{11} - Np_{12} (Px_2 + Np_{22} + Ng_{11} - Ng_{12} (Px_3 + Ng_{22})^{-1} Np_{21})^{-1} \cdot [Up_1 - Np_{12} (Px_2 + Np_{22} + Ng_{11} - Ng_{12} (Px_3 + Ng_{22})^{-1} Ng_{21})^{-1} \cdot (Up_2 + Ug_1 - Ng_{12} (Px_3 + Ng_{22})^{-1} Ug_2)] \quad (17)$$

where

$$Np_{ij} = A_{pi}^T [B_p P_p^{-1} B_p^T]^{-1} A_{pj} \quad (18)$$

$$Ng_{ij} = A_{gi}^T P_g A_{gj} \quad (19)$$

$$Up_i = A_{pi}^T [B_p P_p^{-1} B_p^T]^{-1} W_p \quad (20)$$

$$Ug_i = A_{gi}^T P_g W_g \quad (21)$$

Px_i are the weight matrices for the approximate values of X_i . A computer program named GEBAT (General Bundle Adjustment Triangulation) has been written using the above model.

TEST RESULTS

USING THE ISP TEST BLOCK

Part of the ISP simulated test block (Anderson and Ramy, 1973) has been used to test the program GEBAT. For this test, 25 photographs were used, each containing 9 points. A few sets of geodetic observations of all the types mentioned, together with certain variances, were simulated by the authors. The different distributions of the observations, as displayed in Figures 1, 2, and 3, were used to study

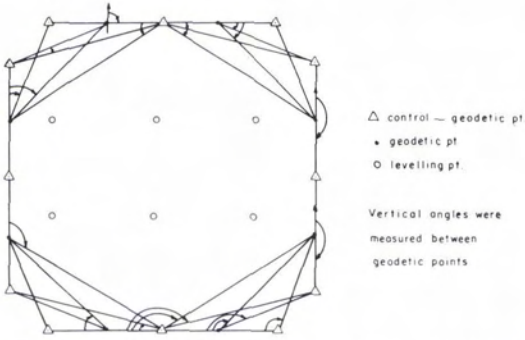


FIG. 1. ISP test block; distribution of geodetic observations; Case #1.

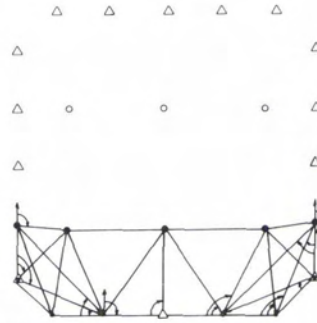


FIG. 2. ISP test block; distribution of geodetic observations; Case #2.

the effect of introducing geodetic observations, when only a few control points are available. Table 1 shows the results of these combined adjustments. The results show a significant improvement when introducing the geodetic observations over the case of using the reduced number of control points only. The improvement depends on the number and distribution of these geodetic observations.

ADJUSTING A DENSE CONTROL NETWORK

The program GEBAT has also been applied to a practical project in an industrial environment (see Figure 4). It consisted of a dense network that contained some 70 points in an area of about 15 by 15 m². Due to the nature of the network and the tight time schedule, that required the adjustment of the network in a relatively short period of time, it was decided to use photogrammetry rather than conventional surveying. The use of surveying would have required thousands of observations and, although the area is small, would have required a long time and thus been rather costly. However, it was easy to level the network with 0.5 mm standard deviation using precision leveling equipment. Furthermore, some 150 space distances had been taped arbitrarily, again with 0.5 mm standard deviation. The required accuracy of the adjusted coordinates was 1 to 2 mm.

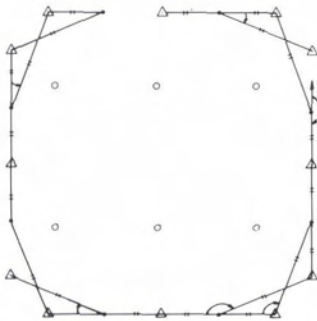


FIG. 3. ISP test block; distribution of geodetic observations; Case #3.

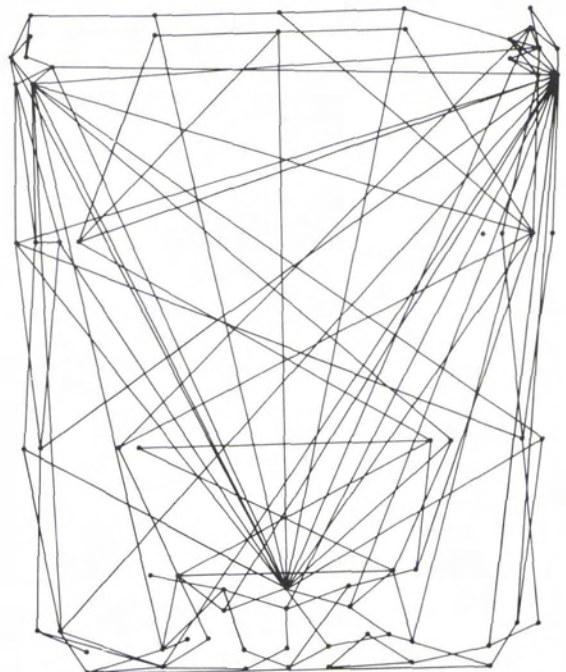


FIG. 4. Layout of industrial control network.

TABLE 1. EFFECT OF GEODETIC OBSERVATIONS (ISP BLOCK) (3-D COORDINATE SYSTEM)

CASE	No. Control		No. of Check Points		Iterations	RMS (check pts.) in m			
	H	V	H	V		X	Y	Z	R
Photogrammetry + full control	20	25	30	25	2	0.42	0.38	0.22	0.61
Photogrammetry + reduced control	12	12	38	38	3	1.20	0.62	0.45	1.43
Photogrammetry + Geodesy (distr. #1)	12	12	38	38	2	0.54	0.32	0.25	0.67
Photogrammetry + Geodesy (distr. #2)	12	12	38	38	2	0.62	0.42	0.28	0.81
Photogrammetry + Geodesy (distr. #3)	12	12	38	38	2	0.73	0.38	0.32	0.88

Due to this high accuracy requirement, the solution had to be planned very carefully, using all the available information as well as the most rigorous techniques. A Wild P-31 phototheodolite with maximum lens distortion of $\pm 4 \mu\text{m}$ and wide angle lens ($f = 100 \text{ mm}$) was employed. Four convergent photographs from the corners of the block were taken, using a crane to raise the exposure station about 10 m above the ground. The block was photographed again from slightly different positions to provide extra coverage to improve the accuracy. The photo scale varied between 1:110 and 1:230. The plate negatives were measured on the Zeiss PSK stereocomparator, and the following adjustments were carried out:

- Combined photogrammetric and spatial distance adjustment using all the available data and self calibration.
- Photogrammetric adjustment only, single coverage (4 photographs) and no additional parameters.
- Same as (b) but with self calibration
- Same as (c) but using all photographs (1 3/4 coverage, seven photographs because one photo did not turn out and had to be discarded).

Adjustment (a) provided the required coordinates for this project, while adjustments (b), (c), and (d) were carried out for research purposes.

Since there is at least one distance observed to each point, the check accuracy is expressed by the RMS of the difference between the distances computed from the adjusted coordinates and the measured distances. The coordinates' accuracy is then equal to the distance accuracy divided by $\sqrt{2}$. The variance covariance matrix of the adjusted coordinates and the corresponding relative error ellipsoid were computed to provide the accuracy of the adjustment.

Table 2 shows the accuracy and the check accuracy for the different adjustments.

These results can be analyzed as follows:

- The combined solution (case a) provided a very high accuracy. The excellent geometry, obtained from the convergent photography, and the availability of 150 spatial distances all over the block provided a complete control for the adjustment. It was also possible to discover some blunders in the distances after performing the adjustment once. Convergency to the solution was achieved after only three iterations, again due to the good geometry.

TABLE 2. ACCURACY OF DIFFERENT ADJUSTMENTS (ALL DIMENSIONS ARE mm)

Case	RMS of Distance Discrepancies	Estimated Coordinate Absolute Error	Mean Variance of Adjusted Coordinates	Semi-major Axis of Error Ellipse (95% c.l.)
a	0.6	0.4	0.8	1.6
b	5.0	3.5	1.7	3.3
c	4.4	3.1	1.7	3.3
d	3.4	2.4	1.4	2.7

TABLE 3. TIME SPENT ON THE PROJECT

Stage	Time(days)	Personnel	Person days
Photography and developing	1/2	2	1
Photo measurements	2	1	2
Preparing the input data	1	1	1
Ground observations	3	2	6
		Total	10

As evident from Figure 4, a trilateration solution was impossible for this case, in spite of the large redundancy in places.

- The large difference in accuracy between case (a) and the other cases is understandable. This is mainly due to the large difference in control, or constraints, between them.

- The improvement by using self calibration was only by a factor 1.14, which may be due to the good quality of the camera and photography. The improvement of 0.4 mm in coordinate errors is equivalent to about 2.5 μm in photo scale (the maximum lens distortion for this camera is 4 μm).

- Multiple coverage improved the results by a factor 1.30. The expected improvement (see also [3]) for double coverage is $\sqrt{2}$ or 1.41 times, but in this project the second coverage was only 3/4 of the first, and thus the expected improvement is 1.31, which was almost achieved practically.

- The standard deviation of the adjusted coordinates gives a good indication of the accuracy. At the 95 percent confidence level, the semi-major axes of the error ellipse is reliable for case (c) and (d). For case (b), some systematic errors existed, and this caused the check error to be slightly outside the error ellipse.

- Considering the cost of this project, the time spent was as shown in Table 3.

Furthermore, the program GEBAT requires one minute per run. An additional run is needed for blunder detection and, thus, a total of two minutes CPU (central processing unit) time is the minimum requirement. The effective run time will be about six minutes. The additional costs for equipment rental and glass plates are small.

To obtain the same results by surveying means, three days (items 1 and 2) could be saved, but at the expense of at least two weeks of field observations, and several days of data preparation. There would be approximately the same computational effort and more instrument rental. Besides the time involved, which could seriously affect the overall production planning, it is safe to say that conventional surveying would have been more expensive by at least a factor two to three.

CONCLUDING REMARKS

As shown in the test results as well as for the practical application in industry, a rigorous simultaneous bundle adjustment using geodetic observations such as distances directly provides an excellent alternative to ground surveying, even if the accuracy requirements are very high. With the inclusion of additional parameters for self calibration, the potentials of photogrammetry are fully explored. Thus, we have a powerful measuring tool that can replace hundreds of angular measurements, not to mention the common advantages of photogrammetry, such as instantaneous, complete, and permanent recording of a situation.

REFERENCES

Anderson, J. M., and E. H. Ramey, 1973. Analytical Block Adjustment, *Photogrammetric Engineering*, V. 39, No. 10, p. 1087.

El Hakim, S. F., 1979. *Potentials and Limitations of Photogrammetry for Precision Surveying*, Ph.D. dissertation, University of New Brunswick, Fredericton.

El Hakim, S. F., and W. Faig, 1977. Compensation of Systematic Image Errors Using Spherical Harmonics, ASP Fall Tech. Meeting, Little Rock, Ark.

Fubara, D., 1972. Three-dimensional Adjustment of Terrestrial Geodetic Networks, *Canadian Surveyor*, V. 26, No. 4.

Kenefick, J. F., et al., 1978. Bridging with Independent Horizontal Control, *Photogrammetric Engineering and Remote Sensing*, V. 44, No. 6, pp 668-695.

Vincenty, T., 1973. *Three-Dimensional Adjustment of Geodetic Networks*, DMAAC Geodetic Survey Squadron, Wyoming.

Wong, K., and G. Elphinstone, 1971. *Simultaneous Adjustment of Photogrammetric and Geodetic Observations (SAPGO)*, Civil Engg. Studies, Photogrammetry Series No. 30, University of Illinois, Urbana—Champaign.

———1972. Aerotriangulation by SAPGO, *Photogrammetric Engineering*, V. 38, No. 8.

(Received 11 December 1979; revised and accepted 14 July 1980)